Offline Recursive Identification of Electrical Parameters of VSI-Fed Induction Motor Drives

Siddavatam Ravi Prakash Reddy, *Student Member, IEEE*, and Umanand Loganathan

***Abstract*—Accurate estimation of electrical parameters of voltage-source-inverter-fed induction machine (IM) drives is very important while employing high-dynamic-performance control schemes, such as vector control. Parameter estimation schemes reported in the literature can estimate only four parameters (R_s, L_{ss}, σ, and τ_r) independently out of five electrical parameters (R_s, R_r, $L_{\sigma s}$, $L_{\sigma r}$, and L_m), when the core loss resistance is neglected. All the five parameters are not independently identified. This article proposes a parameter estimation method that independently identifies all the six electrical parameters (R_s, R_r, R_c, $L_{\sigma s}$, $L_{\sigma r}$, and L_m) of the IM, including the core loss resistance. Besides, the variation of core loss resistance with frequency is also discussed in this article. The Kalman filter algorithm is used to estimate machine parameters in the proposed method. In the proposed method, a sine-triangle pulsewidth modulation signal is used as input excitation, instead of pseudorandom binary sequence signals. The proposed estimation method is validated using both simulation and experimental results.**

***Index Terms*—Induction machine (IM), Kalman filter, parameter estimation, recursive least squares (RLS) method.**

NOMENCLATURE

R_s	Stator resistance.
R_r	Rotor resistance.
R_c	Core loss resistance.
$L_{\sigma s}$	Stator leakage inductance.
L_m	Mutual inductance.
L_{ss}	Stator self-inductance ($L_{\sigma s} + L_m$).
$L_{\sigma r}$	Rotor leakage inductance.
L_{rr}	Rotor self-inductance ($L_{\sigma r} + L_m$).
τ_r	Rotor time constant (L_{rr}/R_r).
σ	Leakage factor ($1 - L_m^2/L_{ss}L_{rr}$).
$i_{s\alpha}$	α-axis component of stator current.
$v_{s\alpha}$	α-axis component of stator voltage.
$\psi_{r\alpha}$	α-axis component of rotor flux linkage.
$i_{m\alpha}$	α-axis component of magnetizing current.
ω_r	Electrical rotor speed.
ω_s	Speed of synchronously rotating (dq) frame.

Manuscript received September 23, 2019; revised December 4, 2019 and February 3, 2020; accepted March 3, 2020. Date of publication March 6, 2020; date of current version June 23, 2020. Recommended for publication by Associate Editor N. R. Zargari. *(Corresponding author: Siddavatam Ravi Prakash Reddy.)*

The authors are with the Department of Electronic Systems Engineering, Indian Institute of Science, Bangalore 560012, India (e-mail: sraviprakash4@gmail.com; lums@iisc.ac.in).

Color versions of one or more of the figures in this article are available online at http://ieeexplore.ieee.org.

Digital Object Identifier 10.1109/TPEL.2020.2978932

I. INTRODUCTION

ESTIMATION of machine parameters has become an integral part of induction motor (IM) drives in many applications, including electric vehicles and servomechanisms [1]. Precise knowledge of these parameters becomes very important in high-dynamic-performance control of IMs. If the machine parameters are not accurately estimated, it can lead to detuning effects and thus resulting in the deterioration of vector-controlled IM drives [2].

Various parameter estimation techniques are reported in [3]–[8]. Lee *et al.* [3] propose a standstill identification method using integral calculations to identify the rotor time constant and the magnetizing inductance of the IM. A self-commissioning procedure to identify only four electrical parameters of the IM is presented in [4]. Here, it is assumed that the stator and rotor leakage inductances are equal. Khambadkone and Holtz [5] present a self-commissioning scheme suitable for the vector control operation of IM drives. Parameter identification using a prediction-error-based method for the sensorless operation of IM drives is proposed in [6]. Excitation signal design for pseudo-random binary sequence (PRBS) signals based on the responses of the step voltage test is presented in this article. Carraro and Zigliotto [7] present a self-commissioning method to identify the parameters of the equivalent circuit of the inverter-fed IM at standstill, compensating for nonlinearities in the inverter. A self-commissioning scheme to identify the magnetization characteristic of the IM for rotor field-oriented control of the IM is discussed in [8].

Recursive least squares (RLS)-based parameter estimation methods have also been reported in [9]–[12]. A parameter identification scheme to estimate four electrical parameters (R_s, L_{ss}, σ, and τ_r) of the IM drive using the least squares principle is proposed in [9]. Stator and rotor field-oriented models of the IM obtained using an extended Kalman filter are presented in [10]. A parameter identification scheme using a vector construction method based on the RLS algorithm is proposed in [11] to estimate four parameters of the IM. An online rotor time constant identification scheme using a linear least squares estimator is discussed in [12].

Estimation of stator and rotor resistances for a speed sensorless operation of IM drives is reviewed in [13]. In this article, the dynamics of the IM are represented in adaptive observer (AO) form to estimate the resistances. The proposed AO form in [13] is further improved in [14], eliminating the need for differentiation of stator currents. In [15], Foti *et al.* present a parameter estimation scheme to identify the stator resistance

and the rotor time constant, by injecting the sinusoidal signal of low frequency to the reference current. A unified model based on a model reference adaptive system to estimate the rotor time constant for indirect field-oriented control of the IM drive is presented in [16].

In all the aforementioned methods, core loss resistance is neglected during the estimation process. Neglecting the iron loss affects the estimation of resistive parameters [17] and also results in the detuning of vector-controlled schemes [18]. Besides, all the five electrical parameters are not obtained individually, when R_c is neglected.

The standstill ($\omega_r = 0$) model of the IM in the stationary reference frame ($\omega_s = 0$) in the continuous domain, when R_c is neglected, is given as follows [6]:

$$\frac{i_{s\alpha}(s)}{v_{s\alpha}(s)} = \frac{\tau_r s + 1}{\sigma\tau_r L_{ss} s^2 + (L_{ss} + \tau_r R_s)s + R_s}. \tag{1}$$

The corresponding discrete domain transfer function of (1), obtained using Euler's forward rule, is given as

$$\frac{i_{s\alpha}(z)}{v_{s\alpha}(z)} = \frac{b_1 z^{-1} + b_2 z^{-2}}{1 + a_1 z^{-1} + a_2 z^{-2}}. \tag{2}$$

It can be inferred from (2) that only four coefficients can be identified from the IM model, when R_c is neglected. The coefficients b_1, b_2, a_1, and a_2 that can be identified using the RLS algorithm are given as follows [6]:

$$\begin{bmatrix} b_1 \\ b_2 \\ a_1 \\ a_2 \end{bmatrix} = \begin{bmatrix} \dfrac{T_s}{\sigma L_{ss}} \\ -\dfrac{T_s}{\sigma L_{ss}} + \dfrac{T_s^2}{\sigma L_{ss}\tau_r} \\ -2 + \dfrac{(\tau_r R_s + L_{ss})T_s}{\sigma L_{ss}\tau_r} \\ 1 - \dfrac{(\tau_r R_s + L_{ss})T_s}{\sigma L_{ss}\tau_r} + \dfrac{R_s T_s^2}{\sigma L_{ss}\tau_r} \end{bmatrix} \tag{3}$$

where T_s is the sampling time. Thus, it can be inferred from (3) that there are four equations and five unknowns. It can be further inferred that the four independent parameters that can be identified are R_s, L_{ss}, σ, and τ_r. Hence, independent identification of all the five electrical parameters is not possible, when the IM is modeled neglecting the effect of R_c.

Input excitation used in the recursive identification process is yet another crucial aspect. The supply voltage (input excitation signal) used in the parameter estimation process has to satisfy the conditions of persistency of excitation to ensure the convergence of parameters [6]. PRBS signals are commonly used as input excitation signals [6], [19]–[21], as these very well meet the conditions of persistency of excitation. In the proposed method, the sine-triangle pulsewidth modulation (SPWM) signal is used as input excitation signal. The advantage is that SPWM pulses are very easy to generate using a voltage-source inverter (VSI) when compared to that of PRBS signals. The persistency of excitation conditions for SPWM pulses is proved in Section III.

Thus, a standstill parameter estimation method is proposed in this article, which can identify all the six electrical parameters simultaneously. The Kalman filter algorithm is used in the proposed method to estimate machine parameters. The main contributions of this article include the following.

1) All the six electrical parameters of the IM can be obtained individually with the proposed method.
2) For input excitation in the proposed method, SPWM pulses, which are much easier to implement than PRBS signals, are used. The order of persistency of excitation is more for SPWM pulses, when compared to PRBS signals, resulting in faster convergence of parameters.
3) While estimating machine parameters, no assumption is made on any of the parameters.
4) As core loss resistance is a function of frequency, a generalized expression is obtained to evaluate R_c at any given frequency.

The rest of this article is organized as follows. Section II discusses about the proposed identification method. The generalized expression for R_c at any given frequency is also obtained in this section. The persistency of excitation conditions for SPWM pulses is proved in Section III. The simulation results for the estimation of machine parameters using the Kalman filter algorithm are presented in Section IV. The experimental results for the proposed method of identification are presented in Section V. Finally, Section VI concludes this article.

II. Proposed Identification Method

It is inferred from the previous section that the standstill model of the IM in the z-domain, given by (2), contains only four coefficients. Thus, only four independent parameters can be identified out of the five parameters, when R_c is neglected.

This section presents the identification of all the six electrical parameters independently, considering the impact of R_c. It may be noted that the core loss is modeled as resistance in parallel with the mutual inductance. Moreover, as R_c varies with fundamental frequency, the evaluation of R_c at different fundamental frequencies is also presented in this section.

A. Standstill Model of the IM Including R_c

Since the estimation of machine parameters is done at standstill ($\omega_r = 0$), the equations of the IM in the stationary reference frame ($\omega_s = 0$) at standstill, corresponding to the α-axis, are given as follows [22]:

$$\begin{aligned} \frac{di_{s\alpha}}{dt} &= -\frac{(R_s + R_c)i_{s\alpha}}{L_{\sigma s}} - \frac{R_c\psi_{r\alpha}}{L_{\sigma s}L_{\sigma r}} + \frac{R_c L_{rr} i_{m\alpha}}{L_{\sigma s}L_{\sigma r}} + \frac{v_{s\alpha}}{L_{\sigma s}} \\ \frac{d\psi_{r\alpha}}{dt} &= -\frac{R_r\psi_{r\alpha}}{L_{\sigma r}} + \frac{L_m R_r i_{m\alpha}}{L_{\sigma r}} \\ \frac{di_{m\alpha}}{dt} &= \frac{R_c i_{s\alpha}}{L_m} + \frac{R_c\psi_{r\alpha}}{L_m L_{\sigma r}} - \frac{R_c L_{rr} i_{m\alpha}}{L_m L_{\sigma r}}. \end{aligned} \tag{4}$$

It may be noted that the effect of magnetic saturation is not considered in the model. The standstill equivalent circuit of the IM is shown in Fig. 1.

By applying the Laplace transform to the equations in (4), the s-domain transfer function of $i_{s\alpha}(s)$ to $v_{s\alpha}(s)$ can be obtained as

$$\frac{i_{s\alpha}(s)}{v_{s\alpha}(s)} = \frac{N_2 s^2 + N_1 s + N_0}{D_3 s^3 + D_2 s^2 + D_1 s + D_0} \tag{5}$$

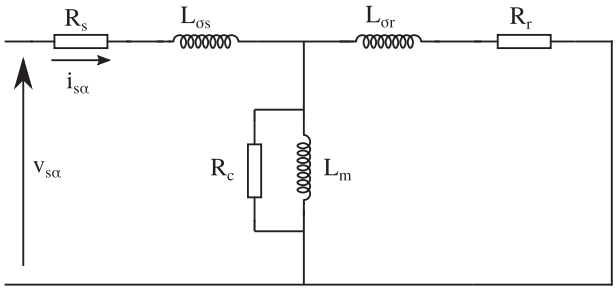

Fig. 1. Equivalent circuit of the IM at standstill.

where the coefficients of the above transfer function are given as

$$N_2 = \frac{L_m L_{\sigma r}}{R_r}$$
$$N_1 = L_m + \frac{R_c L_{rr}}{R_r}$$
$$N_0 = R_c$$
$$D_3 = \frac{L_m L_{\sigma r} L_{\sigma s}}{R_r}$$
$$D_2 = \frac{L_m L_{\sigma r}(R_s + R_c)}{R_r} + \left(L_m + \frac{R_c L_{rr}}{R_r}\right) L_{\sigma s}$$
$$D_1 = \left(L_m + \frac{R_c L_{rr}}{R_r}\right) R_s + R_c L_{\sigma s} + L_m R_c$$
$$D_0 = R_c R_s. \tag{6}$$

Thus, the corresponding discrete-time transfer function of $i_{s\alpha}(z)$ to $v_{s\alpha}(z)$ obtained using Euler's forward rule with a sampling time of T_s is obtained as

$$\frac{y(z)}{u(z)} = \frac{i_{s\alpha}(z)}{v_{s\alpha}(z)} = \frac{n_1 z^{-1} + n_2 z^{-2} + n_3 z^{-3}}{1 + d_1 z^{-1} + d_2 z^{-2} + d_3 z^{-3}} \tag{7}$$

where the coefficients of the z-domain transfer function are related to the coefficients of the s-domain transfer function, as follows:

$$n_1 = \frac{N_2}{D_3} T_s$$
$$n_2 = -2\frac{N_2}{D_3} T_s + \frac{N_1}{D_3} T_s^2$$
$$n_3 = \frac{N_2}{D_3} T_s - \frac{N_1}{D_3} T_s^2 + \frac{N_0}{D_3} T_s^3$$
$$d_1 = -3 + \frac{D_2}{D_3} T_s$$
$$d_2 = 3 - 2\frac{D_2}{D_3} T_s + \frac{D_1}{D_3} T_s^2$$
$$d_3 = -1 + \frac{D_2}{D_3} T_s - \frac{D_1}{D_3} T_s^2 + \frac{D_0}{D_3} T_s^3. \tag{8}$$

Thus, it can be observed that (7) is a third-order transfer function (contains six coefficients), unlike (2), which is only a second-order transfer function (contains four coefficients). This is due to the fact that when the IM model is considered, including R_c, the order of the system increases from 2 to 3. All these six coefficients present in (7) can be estimated using the Kalman filter algorithm.

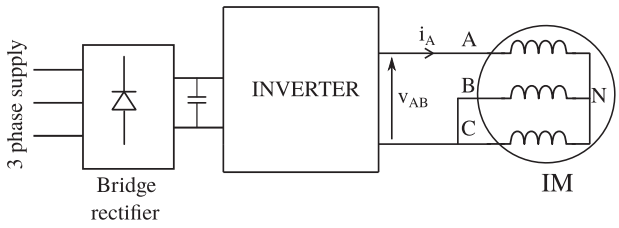

Fig. 2. Block diagram showing the inverter-fed IM drive system.

The process of estimating the z-domain transfer function's coefficients using the Kalman filter algorithm is discussed in the following subsection.

B. Parameter Estimation

The standstill operation for the parameter estimation process is achieved by shorting B and C terminals and applying single phase excitation to the A and B terminals of the IM, as shown in Fig. 2. SPWM pulses are generated by comparing a sinusoidal modulating signal of particular frequency (say 50 Hz) with triangular carrier and is given as input excitation (V_{AB}) to the IM.

The input voltage (V_{AB}) and the observed current (i_A) are sampled with a sampling time of T_s. Let $y(k)$ and $u(k)$ represent the actual values of i_A and V_{AB} at the kth sampling instant, respectively.

The method of parameter estimation is addressed as an optimization problem, in which the response of the system (IM) to a given input is used to estimate the unknown parameters of the IM. Thus, the estimated value of output at the kth sampling instant ($y_{\text{est}}(k)$), which depends on the previous samples of input and output is given by the following expression:

$$y_{\text{est}}(k) = C^T(k)\theta \tag{9}$$

where θ is the parameter estimate vector and $C^T(k)$ denotes the transpose of vector $C(k)$, which contains the previous samples of $u(k)$ and $y(k)$.

The z-domain transfer function given in (7) is converted into a difference equation, which is given as

$$y_{\text{est}}(k) = n_1 u(k-1) + n_2 u(k-2) + n_3 u(k-3) - d_1 y(k-1) - d_2 y(k-2) - d_3 y(k-3). \tag{10}$$

Comparing (10) with (9), the above equation is rewritten as follows:

$$y_{\text{est}}(k) = C^T(k)\theta = \begin{bmatrix} u(k-1) \\ u(k-2) \\ u(k-3) \\ -y(k-1) \\ -y(k-2) \\ -y(k-3) \end{bmatrix}^T \begin{bmatrix} n_1 \\ n_2 \\ n_3 \\ d_1 \\ d_2 \\ d_3 \end{bmatrix}. \tag{11}$$

It can be seen from (11) that the parameter estimate vector θ contains the six coefficients of the z-domain transfer function.

Thus, using the Kalman filter algorithm, the parameter estimate vector θ can be obtained such that the error between the actual output and the estimated output is minimized. The implementation of the Kalman filter algorithm is discussed in the following.

The Kalman filter algorithm is a recursive algorithm, which estimates the optimal values of parameters, such that the objective function given by the following equation is minimized:

$$J(\theta) = \sum_{k=1}^{N} \left(y(k) - y_{\text{est}}(k)\right)^2. \tag{12}$$

The following set of equations summarizes the implementation of the Kalman filter algorithm:

$$\begin{aligned}
\theta(k) &= \theta(k-1) + G(k)\left(y(k) - y_{est}(k)\right)\\
y_{\text{est}}(k) &= C^T(k)\theta(k-1)\\
G(k) &= Q(k)C(k)\\
Q(k) &= \frac{P(k-1)}{R + C^T(k)P(k-1)C(k)}\\
P(k) &= P(k-1) - \frac{P(k-1)C(k)C^T(k)P(k-1)}{R + C^T(k)P(k-1)C(k)}
\end{aligned} \tag{13}$$

where P represents the parameter covariance matrix and $R\,(>0)$ represents process noise covariance, respectively.

The six electrical parameters (R_s^e, R_r^e, R_c^e, $L_{\sigma s}^e$, $L_{\sigma r}^e$, and L_m^e) of the IM to be estimated can be expressed as function of the elements of the parameter estimate vector θ, as discussed in the following subsection.

C. Estimation of Machine Parameters

From (6) and (8), the electrical parameters of the IM can be expressed in terms of elements of the parameter vector θ as follows:

$$\begin{aligned}
R_s^e &= \frac{1 + d_1 + d_2 + d_3}{n_1 + n_2 + n_3}\\
L_{\sigma s}^e &= \frac{T_s}{n_1}\\
L_m^e &= \frac{T_s(d_2 + 2d_1 + 3)}{(n_1 + n_2 + n_3)} - \frac{(n_2 + 2n_1)T_s R_s^e}{(n_1 + n_2 + n_3)} - L_{\sigma s}^e\\
R_c^e &= \frac{(d_1 + 3)}{n_1} - R_s^e - \frac{L_{\sigma s}^e(n_2 + 2n_1)}{n_1 T_s}\\
\frac{L_{\sigma r}^e}{R_r^e} &= \frac{T_s^3 R_c^e}{L_m^e L_{\sigma s}^e(n_1 + n_2 + n_3)}\\
R_r^e &= \frac{L_m^e}{\frac{T_s(n_2+2n_1)}{(n_1+n_2+n_3)} - \frac{L_m^e}{R_c^e} - \frac{L_{\sigma r}^e}{R_r^e}}\\
L_{\sigma r}^e &= \frac{L_{\sigma r}^e}{R_r^e} * R_r^e.
\end{aligned} \tag{14}$$

Thus, all the parameters of the IM can be obtained using the Kalman filter algorithm, corresponding to the input excitation of 50-Hz fundamental frequency.

D. Estimation of R_c at Different Frequencies

The variation of core loss (P_c) in the IM with frequency, keeping flux constant, is given as [23]

$$P_c = \frac{V_{c,f}^2}{R_{c,f}} = Af + Bf^2 \tag{15}$$

where $R_{c,f}$ and $V_{c,f}$ represent the core loss resistance and the rms value of voltage across core loss resistance at a given frequency fundamental "f."

Thus, it is inferred from (15) that, to estimate the value of R_c at any given frequency, it is required to obtain the values of two constants, namely A and B. These constants can be evaluated by exciting the IM with another sinusoidal voltage of different amplitude and frequency, keeping the ratio V/f constant. The voltage across the core loss resistance can be obtained by subtracting the drop across stator resistance and leakage inductance from the stator voltage. Thus, the following relation is inferred:

$$\frac{V_{c,f}}{f} = K \tag{16}$$

where K denotes the V/f ratio.

Using (15) and (16), the expression for core loss resistance is obtained as

$$R_{c,f} = \frac{f}{A' + B'f} \tag{17}$$

with

$$A' = \frac{A}{K^2}, \qquad B' = \frac{B}{K^2}. \tag{18}$$

Thus, the constants A' and B' can be obtained by running the Kalman filter algorithm and evaluating core loss resistance at two different frequencies (say f_1 and f_2). The values of A' and B' are obtained from (17) as follows:

$$\begin{aligned}
A' &= \frac{(R_{c,f_1} - R_{c,f_2})f_1 f_2}{(f_1 - f_2)R_{c,f_1}R_{c,f_2}}\\
B' &= \frac{(R_{c,f_2}f_1 - R_{c,f_1}f_2)}{(f_1 - f_2)R_{c,f_1}R_{c,f_2}}
\end{aligned} \tag{19}$$

where R_{c,f_1} is the core loss resistance evaluated at frequency f_1 and R_{c,f_2} is the core loss resistance evaluated at frequency f_2.

Thus, once the values of A' and B' are obtained, the value of core loss resistance at any given frequency can be found out using (17). It may be noted that (17) cannot be used to determine core loss resistance at zero frequency, as this results in an indeterminate value ($\frac{0}{0}$ form) for K, as can be inferred from (16).

III. Persistency of Excitation

The selection of excitation input is very important for the process of parameter estimation. The input should be persistently exciting in order to ensure the correct convergence of

parameters [24]. The order of persistency of excitation required for a given input signal is discussed in the following.

Consider the following transfer function:

$$\frac{y(z)}{u(z)} = \frac{p_1 z^{-1} + p_2 z^{-2} + \cdots + p_m z^{-m}}{1 + q_1 z^{-1} + q_2 z^{-2} + \cdots + q_n z^{-n}} \quad (n > m). \quad (20)$$

For the transfer function given in (20), in order to ensure the convergence of parameters, the excitation input should be persistently exciting of order at least $(m+n)$. Thus, for the proposed identification scheme, the input $u(t)$ should be persistently exciting of order at least 6. This is because the transfer function in the proposed identification scheme has $m = 3$ and $n = 3$.

PRBS signals are popular signals for the identification of system dynamics. In this article, the SPWM signal is used as input excitation. The advantage of using SPWM signals is that these can be very easily generated using the VSI, when compared to that of PRBS signals.

Now, we prove that the SPWM signals can easily meet the persistency of excitation conditions for the proposed identification scheme (i.e., we have to prove that the order of persistency of excitation for SPWM signals is at least 6). A signal $u(t)$ is said to be persistently exciting of order "N" if it has at least "N" nonzero points in $\phi_u(\omega)$, where $\phi_u(\omega)$ represents the Fourier transform of the autocorrelation function of $u(t)$. Thus, the expression for $\phi_u(\omega)$ is given by

$$\phi_u(\omega) = \sum_{\tau=-\infty}^{\infty} R(\tau) e^{-j\omega\tau} \quad (21)$$

where $R(\tau)$ is called the autocorrelation function, and the expression for $R(\tau)$ is given by

$$R(\tau) = \lim_{T\to\infty} \frac{1}{T} \int_{t=0}^{T} f(t+\tau) f(t) dt \quad (22)$$

with T being the time period of $f(t)$.

The expression for the SPWM waveform, $u(t) = V_{AB}(t)$, can be obtained from double Fourier integral analysis [25], as given in (23). Let the sinusoidal modulating wave be represented by $m(t) = M\sin(\omega_m t)$, with M $(0 \le M \le 1)$ being the modulation index. Let the amplitude of triangular carrier be ± 1.

$$u(t) = V_{AB}(t) = \frac{MV_{\rm DC}}{2}\sin(\omega_m t) + \sum_{m=1}^{\infty} a_m \sin(m\omega_c t) + \sum_{m=1}^{\infty} \sum_{\substack{n=-\infty \\ (n\neq 0)}}^{\infty} b_m \sin(m\omega_c t + n\omega_m t)$$

$$\text{where } a_m = \frac{2V_{\rm DC}}{m\pi} J_0\left(\frac{m\pi M}{2}\right) \sin\left(\frac{m\pi}{2}\right)$$

$$b_m = \frac{2V_{\rm DC}}{m\pi} J_n\left(\frac{m\pi M}{2}\right) \sin\left(\frac{(m+n)\pi}{2}\right). \quad (23)$$

$J_0(\frac{m\pi M}{2})$ and $J_n(\frac{m\pi M}{2})$ represent the Bessel's functions of order 0 and n, respectively. ω_m $(=2\pi f_m)$ and ω_c $(=2\pi f_c)$ represent the frequencies of sinusoidal modulating wave and triangular carrier, respectively. $V_{\rm DC}$ represents the dc-link voltage.

The expression of $R(\tau)$ for $v_{RY}(t)$, evaluated using (22), is given as

$$R(\tau) = \frac{k^2}{2}\cos(\omega_m \tau) + \sum_{m=1}^{\infty} \frac{a_m^2}{2}\cos(m\omega_c \tau) + \sum_{m=1}^{\infty} \sum_{\substack{n=-\infty \\ (n\neq 0)}}^{\infty} \frac{b_m^2}{2}\cos(m\omega_c \tau + n\omega_m \tau). \quad (24)$$

Similarly, the expression for $\phi_u(\omega)$, evaluated using (21), is obtained as

$$\phi_u(\omega) = \frac{k^2}{2}\left[\delta(\omega-\omega_m) + \delta(\omega+\omega_m)\right] + \sum_{m=1}^{\infty} \frac{a_m^2}{2}\left[\delta(m\omega - m\omega_c) + \delta(m\omega + m\omega_c)\right] + \sum_{m=1}^{\infty} \sum_{\substack{n=-\infty \\ (n\neq 0)}}^{\infty} \frac{b_m^2}{2}\left[\delta(m(\omega-\omega_c) + n(\omega-\omega_m)) + \delta(m(\omega+\omega_c) + n(\omega+\omega_m))\right]. \quad (25)$$

It can be inferred from (25) that $\phi_u(\omega)$ is nonzero for the following points: 1) $\omega = \pm\omega_m$; 2) $\omega = \pm m\omega_c (m = 1, 3, 5, \ldots)$; and 3) $\omega = \pm m\omega_c \pm n\omega_m (m + n = 1, 3, 5, \ldots$ and $n \neq 0)$. Thus, $\phi_u(\omega)$ is seen to be nonzero for at least six points, and hence, the SPWM signal used is proved to be persistently exciting for the proposed identification scheme.

IV. Simulation Results

Simulations are carried out using MATLAB Simulink to validate the proposed identification scheme. The model of the IM used for simulation verification is based on (4). The parameters of the machine model used are as follows: $R_s = 2.9\ \Omega$, $R_r = 12.5\ \Omega$, $R_c = 1000\ \Omega$ at 50 Hz, $L_{\sigma s} = 16.1$ mH, $L_{\sigma r} = 6.6$ mH, and $L_m = 369$ mH.

A. Estimation of Machine Parameters Using the Proposed Method

Fig. 3 shows the simulation results for the proposed identification scheme. A sinusoidal modulating wave of frequency 50 Hz is compared with triangular carrier wave of frequency 1 kHz to generate SPWM pulses, as shown in Fig. 3(a). The modulation index (M) used is 0.8. Thus, the SPWM pulses generated are given as input excitation V_{AB} [shown in Fig. 3(b)] during the parameter identification process. The Kalman filter algorithm is used for estimation. The Kalman filter algorithm routine is given as follows.

1) Start with the initial values for the parameter estimate vector θ_0 and the parameter covariance matrix P_0. The initial values θ_0 and P_0 used are given as

$$\theta_0 = [0 \quad 0 \quad 0 \quad 0 \quad 0 \quad 0]^T, \quad P_0 = 10^{-6}.I_6 \quad (26)$$

where I_6 is an identity matrix of order 6×6. The process noise covariance R is set as 0.001.

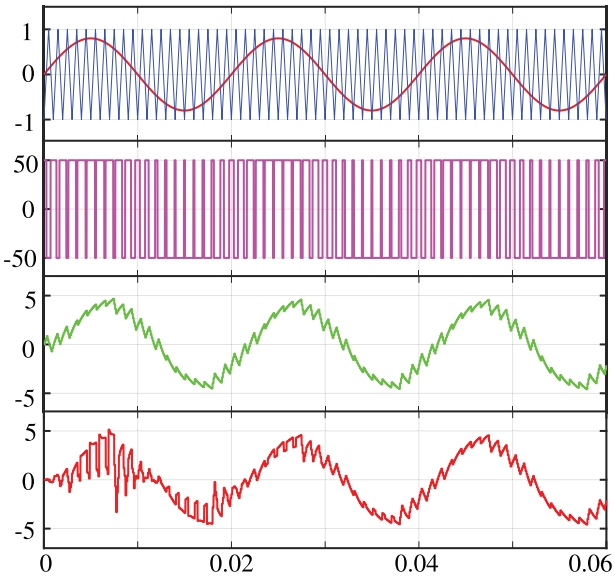

Fig. 3. Simulation results showing On the x-axis: time (seconds). On the y-axis: From top to bottom: (a) Sine wave (50 Hz) compared with triangular carrier of 1 kHz, (b) input excitation voltage in Volts (V_{AB}), (c) actual output in Amperes (y_{act}), and (d) estimated output in Amperes (y_{est}).

TABLE I
ACTUAL AND ESTIMATED PARAMETERS OF THE IM (SIMULATION RESULTS)

Parameter	Units	Actual value	Estimated value
R_s	ohms	2.9	2.893
R_r	ohms	12.5	11.981
R_c	ohms	1000	1056.3
$L_{\sigma s}$	mH	16.1	17.969
$L_{\sigma r}$	mH	6.6	6.289
L_m	mH	369	375.21

2) As the vector $C(k)$, given by (11), contains $u(k-3)$ and $y(k-3)$ terms, the Kalman filter algorithm, given by (13), is executed from the fourth sampling instant ($k=4$).
3) The above step (step 2) is repeated till all the elements in the parameter estimate vector reach steady state.
The actual (y_{act}) and estimated (y_{est}) values of output during the parameter estimation process are shown in Fig. 3(c) and (d), respectively. It can be inferred that the estimated output (y_{est}) of the Kalman filter algorithm differs from the actual output (y_{act}) in the beginning, and finally, both become the same in the steady state.

The simulation results showing the estimation of all the six electrical parameters of the IM are shown in Fig. 4. The estimated and actual values of machine parameters are also listed in Table I.

B. Addition of External Resistance to the Stator Terminals

The proposed method is also verified by adding external resistance to the stator terminals of the IM and measuring the increment in the value of R_s. An external resistance of 1 Ω is added to the stator after some time, and it can be validated from Fig. 5 that the proposed method can track the changes in the value of the stator resistance made. It is observed that the stator resistance has changed from its value of 2.893–3.931 Ω, as shown in Fig. 5.

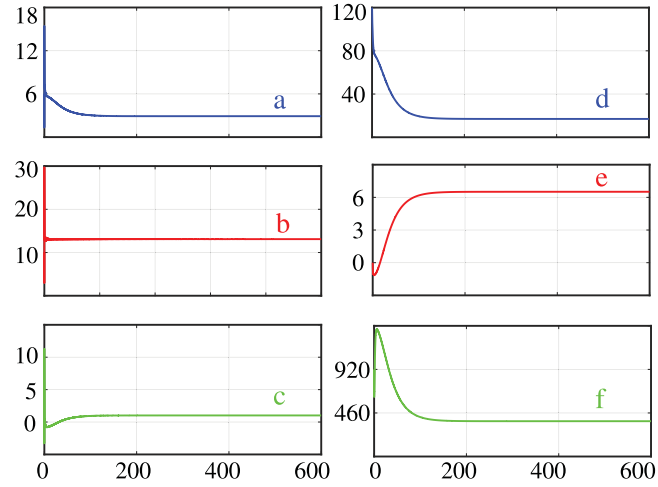

Fig. 4. Simulation results showing the estimation of electrical parameters of the IM. On the x-axis: Iteration number. On the y-axis: (a) Stator resistance (Ω), (b) rotor resistance (Ω), (c) core loss resistance at 50 Hz (kΩ), (d) stator leakage inductance (mH), (e) rotor leakage inductance (mH), and (f) mutual inductance (mH).

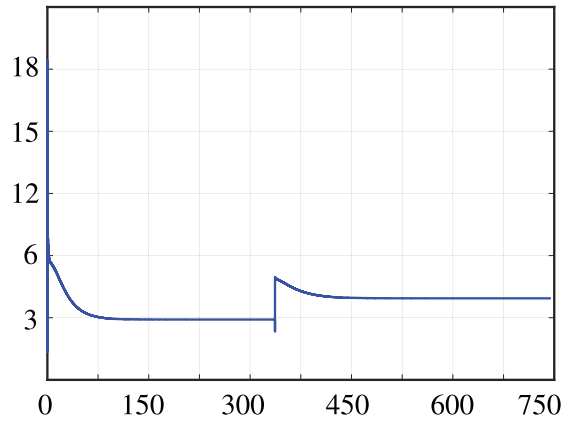

Fig. 5. Simulation results showing the estimation of stator resistance when it is increased from its nominal value of 2.9 to 3.9 Ω. On the x-axis: Iteration number. On the y-axis: Stator resistance (Ω).

V. EXPERIMENTAL RESULTS

A. Hardware Platform

The proposed identification scheme is also experimentally verified on two different machines. The details of both the machines are as follows: Machine 1: 400-V, 1-kW, 2.2-A, three-phase IM; Machine 2: 415-V, 3.7-kW, 7.5-A, three-phase IM. The TMS320F28334 digital signal processor (DSP) is used to implement the control algorithm. The complete experimental setup showing the various parts is shown in Fig. 6. The schematic showing the block diagram of hardware and software platforms is also shown in Fig. 7.

Fig. 6. Hardware setup showing various parts: 1) IM, 2) inverter, 3) sensor board, and 4) DSP board.

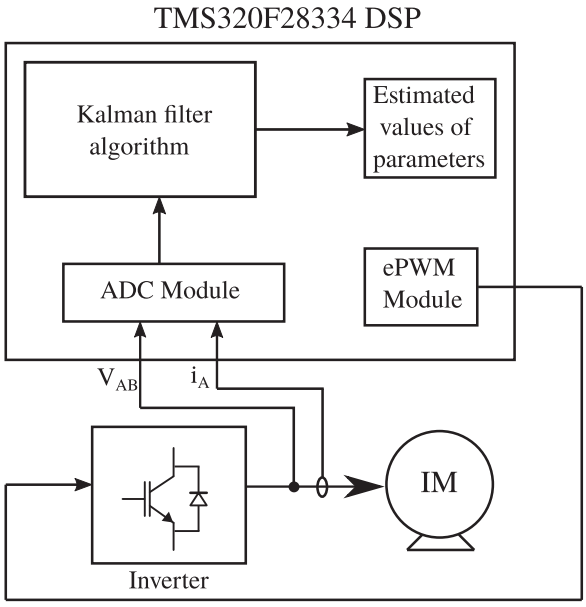

Fig. 7. Block diagram showing the hardware and software platforms for the estimation of machine parameters.

A three-phase two-level inverter using half-bridge insulated-gate bipolar transistor modules (SKM100GB128D) is used to drive the IM. The current (i_A) is sensed using the LA 55-P current transducer, and the input voltage (V_{AB}) is sensed using the LV 20-P voltage transducer. Both the sensed values are taken to an analog-to-digital converter (ADC) of the DSP, and thus, current and voltage samples are obtained.

A sampling time (T_s) of 100 μs is used for parameter estimation. An enhanced pulsewidth modulation module is used to generate SPWM pulses, required for input excitation. The following parameters are considered during the experiment: modulation index $M = 0.8$, modulating frequency $f_m = 50$ Hz, and carrier frequency $f_c = 1$ kHz. The initial values θ_0 are set to zero. P_0 and R used in the experiment are given as

$$P_0 = 10^{-3}.I_6, \qquad R = 0.0001. \tag{27}$$

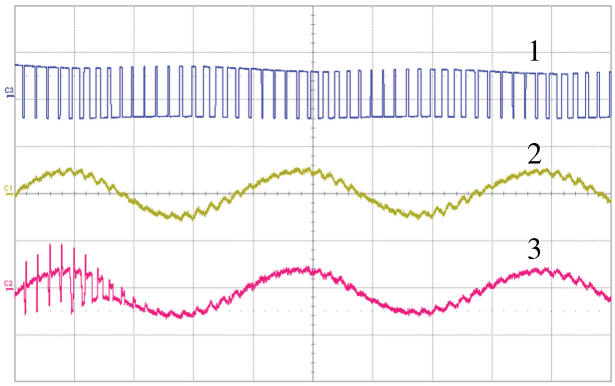

Fig. 8. Experimental results showing the input excitation voltage and actual and estimated outputs using the Kalman filter algorithm. On the x-axis: time (5 ms/div). On the y-axis: 1) Input excitation voltage, V_{AB} (20 V/div), 2) actual output, y_{act} (1 A/div), and 3) estimated output, y_{est} (1 A/div).

TABLE II
ESTIMATED PARAMETERS OF THE IM (EXPERIMENTAL RESULTS)

		Machine 1		Machine 2	
Parameter	Units	Proposed	112-2017	Proposed	112-2017
R_s	ohms	5.412	5.4	4.208	4.2
R_r	ohms	10.342	9.962	5.984	5.28
R_c	ohms	1102.6	1073.3	1400.754	1213.7
$L_{\sigma s}$	mH	26.474	24.14	20.719	16.12
$L_{\sigma r}$	mH	25.632	24.14	15.957	16.12
L_m	H	0.809	0.825	0.512	0.463

B. Experimental Results

1) Estimation of Machine Parameters: The input excitation voltage given and the actual and the estimated outputs (currents) of the Kalman filter algorithm are shown in Fig. 8. These results are shown for machine 1. It can be seen that the estimated output (y_{est}) differs from the actual output (y_{act}) in the beginning, and finally, both become the same in the steady state.

The experimental results showing the estimation of all the six electrical parameters of the IM for machines 1 and 2 are shown in Figs. 9 and 10, respectively. The estimated values of the electrical parameters for both the machines using the proposed method are also tabulated in Table II.

Note that the core loss resistance is estimated at a frequency of 50 Hz. Thus, to get the expression for R_c at any given frequency, the Kalman filter algorithm is executed again, by using modulating wave of different frequency, as discussed in Section II-D. The expression for R_c is obtained in the following subsection.

2) Addition of External Resistance to Stator Terminals: The proposed method is also verified by conducting two more experiments, by adding external resistances (R_{ext}) of 1 and 2 Ω to the stator terminals. This verification will be more convincing, as the real parameters of the machine are difficult to define. Table III summarizes the experiments done on both the machines.

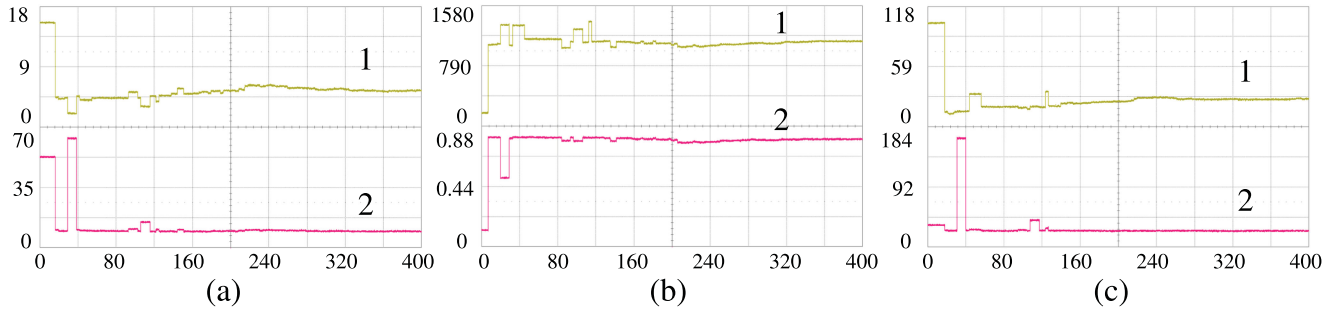

Fig. 9. Experimental results showing the estimation of all the six electrical parameters of machine 1. On the x-axis: Iteration number. On the y-axis: (a) 1. stator resistance (Ω) and 2. rotor resistance (Ω), (b) 1. core loss resistance at 50 Hz (Ω) and 2. mutual inductance (H), (c) 1. stator leakage inductance (mH) and 2. rotor leakage inductance (mH).

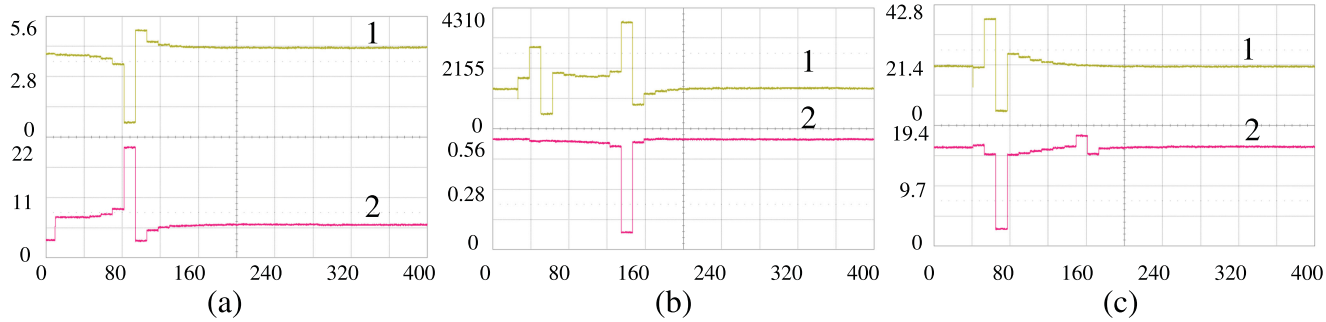

Fig. 10. Experimental results showing the estimation of all the six electrical parameters of machine 2. On the x-axis: Iteration number. On the y-axis: (a) 1. stator resistance (Ω) and 2. rotor resistance (Ω), (b) 1. core loss resistance at 50 Hz (Ω) and 2. mutual inductance (H), (c) 1. stator leakage inductance (mH) and 2. rotor leakage inductance (mH).

TABLE III
ADDITION OF EXTERNAL RESISTANCE (EXPERIMENTAL RESULTS)

	Machine 1		Machine 2	
Ext. resistance	R_s	$R_s + R_{ext}$	R_s	$R_s + R_{ext}$
R_{ext} = 1 Ω	5.412	6.167	4.208	5.103
R_{ext} = 2 Ω	5.412	7.068	4.208	6.312

C. Expression for Core Loss Resistance

The core loss resistances evaluated for machine 1 at two different frequencies of 50 and 20 Hz are obtained as 1102.6 and 572.25 Ω, respectively. Thus, the values of A' and B', obtained from (19), are given as

$$A' = 0.028 \qquad B' = 3.466 \times 10^{-4}. \tag{28}$$

Substituting the values of A' and B', the expression for core loss resistance at any given frequency can be evaluated as

$$R_c \text{ (for machine 1)} = \frac{100f}{2.8 + 0.03466f}. \tag{29}$$

The same experiment is performed on machine 2 as well, and the expression for core loss resistance for machine 2 is obtained as

$$R_c \text{ (for machine 2)} = \frac{100f}{1.94 + 0.032656f}. \tag{30}$$

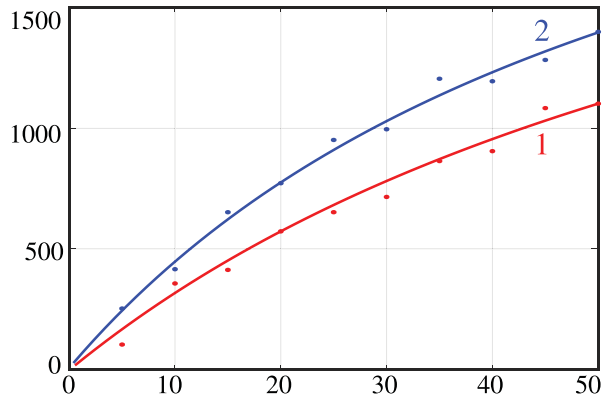

Fig. 11. Result showing the variation of core loss resistance with frequency. Red and blue traces indicate core loss resistance for machines 1 and 2, respectively. On the x-axis: Fundamental frequency (Hz). On the y-axis: core loss resistance (Ω).

The plot showing the variation of core loss resistance with frequency for both the machines is given in Fig. 11. The curves plotted in Fig. 11 are validated by obtaining experimental values of R_c in the frequency range of 5–50 Hz, in discrete intervals of 5 Hz. The values thus obtained are also plotted (as dotted points)

in Fig. 11. It can be inferred that the dotted points closely match with the curves plotted. It may be noted that the equations given in (29) and (30) cannot be used to determine the value of R_c at zero frequency, as this results in an indeterminate value for the value of K. Thus, the curve will be discontinuous at zero frequency.

D. Comparison With the IEEE 112-2017 Standard

The proposed method of parameter estimation is compared with the 112-2017—IEEE Standard Test Procedure for Polyphase Induction Motors and Generators [26]. Table II shows the comparison of estimated electrical parameters for both the machines using the proposed method as well as IEEE 112-2017 methods. It can be inferred that the IEEE 112-2017 standard assumes that the stator and rotor leakage inductances are equal. However, both these leakage inductances can be obtained separately using the proposed estimation method.

VI. Conclusion

A parameter estimation method using the Kalman filter algorithm is presented in this article. The salient feature of the proposed method is that all the six electrical parameters of the IM are identified individually, without making any assumptions. The persistency of excitation conditions for the SPWM signal used is also proved in this article. A generalized expression for core loss resistance at any given frequency is also obtained in this article. The proposed method is validated using both simulation and experimental results.

References

[1] S. A. Odhano, P. Pescetto, H. A. A. Awan, M. Hinkkanen, G. Pellegrino, and R. Bojoi, "Parameter identification and self-commissioning in ac motor drives: A technology status review," *IEEE Trans. Power Electron.*, vol. 34, no. 4, pp. 3603–3614, Apr. 2019.

[2] R. Krishnan and A. S. Bharadwaj, "A review of parameter sensitivity and adaptation in indirect vector controlled induction motor drive systems," *IEEE Trans. Power Electron.*, vol. 6, no. 4, pp. 695–703, Oct. 1991.

[3] S. Lee, A. Yoo, H. Lee, Y. Yoon, and B. Han, "Identification of induction motor parameters at standstill based on integral calculation," *IEEE Trans. Ind. Appl.*, vol. 53, no. 3, pp. 2130–2139, May/Jun. 2017.

[4] C. Concari, G. Franceschini, and C. Tassoni, "Induction drive health assessment in DSP-based self-commissioning procedures," *IEEE Trans. Ind. Electron.*, vol. 58, no. 5, pp. 1490–1500, May 2011.

[5] A. M. Khambadkone and J. Holtz, "Vector-controlled induction motor drive with a self-commissioning scheme," *IEEE Trans. Ind. Electron.*, vol. 38, no. 5, pp. 322–327, Oct. 1991.

[6] J. Ruan and S. Wang, "A prediction error method-based self-commissioning scheme for parameter identification of induction motors in sensorless drives," *IEEE Trans. Energy Convers.*, vol. 30, no. 1, pp. 384–393, Mar. 2015.

[7] M. Carraro and M. Zigliotto, "Automatic parameter identification of inverter-fed induction motors at standstill," *IEEE Trans. Ind. Electron.*, vol. 61, no. 9, pp. 4605–4613, Sep. 2014.

[8] M. Bertoluzzo, G. S. Buja, and R. Menis, "Self-commissioning of RFO IM drives: One-test identification of the magnetization characteristic of the motor," *IEEE Trans. Ind. Appl.*, vol. 37, no. 6, pp. 1801–1806, Nov./Dec. 2001.

[9] K. Wang, J. Chiasson, M. Bodson, and L. M. Tolbert, "An online rotor time constant estimator for the induction machine," *IEEE Trans. Control Syst. Technol.*, vol. 15, no. 2, pp. 339–348, Mar. 2007.

[10] M. Barut, S. Bogosyan, and M. Gokasan, "Speed-sensorless estimation for induction motors using extended Kalman filters," *IEEE Trans. Ind. Electron.*, vol. 54, no. 1, pp. 272–280, Feb. 2007.

[11] Y. He, Y. Wang, Y. Feng, and Z. Wang, "Parameter identification of an induction machine at standstill using the vector constructing method," *IEEE Trans Power Electron.*, vol. 27, no. 2, pp. 905–915, Feb. 2012.

[12] V. Popovic, D. Oros, V. Vasic, and D. Marcetic, "Tuning the rotor time constant parameter of IM using the minimum order recursive linear least square estimator," *IET Electr. Power Appl.*, vol. 13, no. 2, pp. 266–276, 2019.

[13] J. Chen and J. Huang, "Stable simultaneous stator and rotor resistances identification for speed sensorless IM drives: Review and new results," *IEEE Trans. Power Electron.*, vol. 33, no. 10, pp. 8695–8709, Oct. 2018.

[14] J. Chen, J. Huang, and Y. Sun, "Resistances and speed estimation in sensorless induction motor drives using a model with known regressors," *IEEE Trans. Ind. Electron.*, vol. 66, no. 4, pp. 2659–2667, Apr. 2019.

[15] S. Foti, A. Testa, S. De Caro, T. Scimone, and M. Pulvirenti, "Rotor flux position correction and parameters estimation on sensorless multiple induction motors drives," *IEEE Trans. Ind. Appl.*, vol. 55, no. 4, pp. 3759–3769, Jul./Aug. 2019.

[16] P. Cao, X. Zhang, and S. Yang, "A unified-model-based analysis of MRAS for online rotor time constant estimation in an induction motor drive," *IEEE Trans. Ind. Electron.*, vol. 64, no. 6, pp. 4361–4371, Jun. 2017.

[17] D. Chatterjee, "Impact of core losses on parameter identification of three-phase induction machines," *IET Power Electron.*, vol. 7, no. 12, pp. 3126–3136, 2014.

[18] E. Levi, M. Sokola, A. Boglietti, and M. Pastorelli, "Iron loss in rotor-flux-oriented induction machines: Identification, assessment of detuning, and compensation," *IEEE Trans. Power Electron.*, vol. 11, no. 5, pp. 698–709, Sep. 1996.

[19] S. Yaacob and F. A. Mohamed, "Black-box modelling of the induction motor," in *Proc. 37th SICE Annu. Conf. Int. Session Papers*, Jul. 1998, pp. 883–886.

[20] H. Djadi, K. Yazid, and M. Menaa, "Parameters identification of a brushless doubly fed induction machine using PRBS excitation signal for recursive least squares method," *IET Electr. Power Appl.*, vol. 11, no. 9, pp. 1585–1595, Jul. 2017.

[21] J. Holtz and T. Thimm, "Identification of the machine parameters in a vector-controlled induction motor drive," *IEEE Trans. Ind. Appl.*, vol. 27, no. 6, pp. 1111–1118, Nov./Dec. 1991.

[22] E. Levi, "Impact of iron loss on behavior of vector controlled induction machines," *IEEE Trans. Ind. Appl.*, vol. 31, no. 6, pp. 1287–1296, Nov./Dec. 1995.

[23] A. E. Fitzgerald, C. Kingsley, and S. D. Umans, *Electric Machinery*, 5th ed. New York, NY, USA: McGraw-Hill, 1990.

[24] P. E Wellstead and M. B. Zarrop, *Self-Tuning Systems: Control and Signal Processing*. Hoboken, NJ, USA: Wiley, 1991.

[25] D. G. Holmes and T. A. Lipo, *Pulse Width Modulation for Power Converters: Principles and Practice*. Hoboken, NJ, USA: Wiley, 2003.

[26] *IEEE Standard Test Procedure for Polyphase Induction Motors and Generators*, IEEE Standard 112-2017 (Revision of IEEE Standard 112-2004), Feb. 2018, pp. 1–115.

Siddavatam Ravi Prakash Reddy (Student Member, IEEE) received the B.Tech. degree in electrical and electronics engineering from the National Institute of Technology, Calicut, Kozhikode, India, in 2015. He is currently working toward the Ph.D. degree with the Department of Electronic Systems Engineering, Indian Institute of Science, Bangalore, India.

His research interests include power electronic converters, high-performance control, and self-commissioning of induction motor drives for electric vehicle applications.

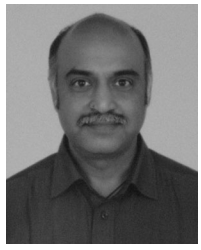

Umanand Loganathan received the bachelor's degree in electronics and communication from Bangalore University, Bangalore, India, in 1987, and the M.Tech. degree in electronics design and the Doctoral degree in control of high-performance induction motor drives from the Indian Institute of Science, Bangalore, in 1989 and 1996, respectively.

He is currently a Professor with the Department of Electronics Systems Engineering, Indian Institute of Science. His research interests include photovoltaic system design, bond graph modeling of power electronic systems, high -performance control of induction motors, designing for reliability, and hybrid electric vehicles.